

Polarized superfluid state in a three-dimensional fermionic optical lattice

A. Koga^a, J. Bauer^b, P. Werner^c, Th. Pruschke^d

^aDepartment of Physics, Tokyo Institute of Technology, Tokyo 152-8551, Japan

^bMax-Planck Institute for Solid State Research, Heisenbergstr. 1, 70569 Stuttgart, Germany

^cTheoretische Physik, ETH Zurich, 8093 Zürich, Switzerland

^dInstitut für Theoretische Physik Universität Göttingen, Göttingen D-37077, Germany

arXiv:1006.4965v1 [cond-mat.quant-gas] 25 Jun 2010

Abstract

We study ultracold fermionic atoms trapped in a three dimensional optical lattice by combining the real-space dynamical mean-field approach with continuous-time quantum Monte Carlo simulations. For a spin-unpolarized system we show results the density and pair potential profile in the trap for a range of temperatures. We discuss how a polarized superfluid state is spatially realized in the spin-polarized system with harmonic confinement at low temperatures and present the local particle density, local magnetization, and pair potential.

Keywords: dynamical mean-field theory, continuous-time quantum Monte Carlo simulation

1. Introduction

Since the successful realization of Bose-Einstein condensation in bosonic ⁸⁷Rb [1] and ²³Na [2] systems, ultracold atoms have attracted considerable interest [3, 4, 5]. One of the most active research areas in this field concerns optical lattice systems, which are generated by subjecting the trapped ultracold atoms to a periodic potential generated by appropriated laser beams [6, 7, 8, 9]. The setups provide clean quantum systems with parameters which can be tuned in a controlled fashion. Remarkable phenomena have been observed such as the phase transition between a Mott insulator and a superfluid in bosonic systems [10]. In the fermionic case, both the superfluid state [11] and the Mott insulating state [12, 13] have been observed. Furthermore, spin imbalanced populations have recently been realized [14, 15], which stimulate further theoretical and experimental investigations on ultracold fermionic systems, and allow to investigate well-known ideas from conventional condensed matter physics.

For the imbalanced system with attractive interactions, interesting ordered ground states have been proposed as the standard s-wave pairing at the Fermi surface is then modified. One of the most prominent candidates is the Fulde-Ferrell-Larkin-Ovchinnikov (FFLO) phase [16, 17], in which Cooper pairs with nonzero total momentum are formed. This phase has been observed in the high field region in CsCoIn₅ [18, 19, 20], and has theoretically been discussed in this compounds [21], as well as cold atoms with imbalanced populations [22, 23]. Another proposed phase is the breached-pair (BP) phase, where both the superfluid order parameter and the magnetization are finite at zero temperature [24, 25, 26, 27, 28]. When one considers three dimensional optical lattice systems at finite temperatures, the naively expected polarized superfluid state may be more stable than the others. However, it is not clear how the polarized superfluid state is realized, and how the pair potential and the

magnetization are spatially distributed in the imbalanced system with a confining potential. Understanding this issue may be important to observe the polarized superfluid state experimentally.

In order to clarify these aspects, we investigate the attractive Hubbard model with imbalanced spin populations and a confining potential. This allows to discuss the effect of the imbalanced spin populations on the superfluid state. By using real-space dynamical mean-field theory (R-DMFT) [29, 30, 31, 32], we study the low temperature properties of the model. Here, we use the continuous-time quantum Monte Carlo (CTQMC) method [33] based on the Nambu formalism as an impurity solver [34]. By calculating the local particle density, local magnetization and pair potential, we clarify how the polarized superfluid state is realized in the spin imbalanced system within the confining potential.

The paper is organized as follows. In Sec. 2, we introduce the model Hamiltonian and summarize various aspects of the R-DMFT. We demonstrate how the superfluid state is realized in a fermionic optical lattice with the confining potential in Sec. 3. A brief summary is given in the last section.

2. Model Hamiltonian and Method

Let us consider ultracold fermionic atoms in an optical lattice with harmonic confinement, which may be described by the following attractive Hubbard Hamiltonian [35, 36, 37, 38, 39, 40, 41, 42],

$$H = \sum_{\langle ij \rangle \sigma} -t c_{i\sigma}^\dagger c_{j\sigma} + \sum_{i\sigma} \left[-(\mu + h\sigma) + V \left(\frac{r_i}{a} \right)^2 \right] n_{i\sigma} - U \sum_i \left[n_{i\uparrow} n_{i\downarrow} - \frac{1}{2} (n_{i\uparrow} + n_{i\downarrow} - 1) \right], \quad (1)$$

where $c_{i\sigma}(c_{i\sigma}^\dagger)$ annihilates (creates) a fermion at the i th site with spin σ and $n_{i\sigma} = c_{i\sigma}^\dagger c_{i\sigma}$. h acts as a magnetic field which allows as to tune the spin population imbalance, μ is the chemical potential, $t(> 0)$ denotes the nearest neighbor hopping and $U(> 0)$ the attractive interaction. V is the curvature of the harmonic potential. The notation $\langle ij \rangle$ indicates that the sum is restricted to nearest neighbors. r_i is the distance measured from the center of the trap and a is the lattice spacing.

The ground-state properties of the Hubbard model on inhomogeneous lattices have been studied theoretically by various methods such as the Bogoljubov-de Gennes (BdG) equations [43], the Gutzwiller approximation [44], the slave-boson mean-field approach [45], variational Monte Carlo simulations [46], and the local density approximation[47]. On the other hand, there are few studies addressing the effect of imbalanced populations beyond the static mean-field approach. The density matrix renormalization group method[48, 49] and the quantum Monte Carlo method[50, 51] are powerful for low dimensional systems, but it may encounter difficulties when applied it to higher dimensional systems. Here we use the R-DMFT approach [29, 30, 31, 32], where local particle correlations are taken into account precisely. This treatment is formally exact for the homogeneous lattice model in infinite dimensions [29, 30, 31, 32] and the method has successfully been applied to some inhomogeneous correlated systems such as the surface [52] or the interface of a Mott insulators [53], and to fermionic atoms [54, 55, 56].

In R-DMFT, the lattice model is mapped to a collection of effective impurity models. The lattice Green function is then obtained via a self-consistency condition imposed on the impurity problems. When one describes the superfluid state in the framework of R-DMFT [29, 30, 31, 32], the lattice Green's function should be represented in the Nambu-Gor'kov formalism. For a system with L lattice sites it is then given by an $(L \times L)$ matrix, where each component consists of a (2×2) matrix as,

$$\begin{aligned} [\hat{G}_{lat}^{-1}(i\omega_n)]_{ij} &= -t\delta_{\langle ij \rangle}\hat{\sigma}_z \\ &+ \delta_{ij}[(i\omega_n + h)\hat{\sigma}_0 + \mu_i\hat{\sigma}_z - \hat{\Sigma}_i(i\omega_n)], \end{aligned} \quad (2)$$

where $i, j = 1, 2, \dots, L$, $\mu_i = \mu - V(r_i/a)^2$, $\hat{\sigma}_z$ is the z component of the Pauli matrix, $\hat{\sigma}_0$ the identity matrix, $\omega_n = (2n + 1)\pi T$ the Matsubara frequency, and T the temperature. $\delta_{\langle ij \rangle}$ is 1 when site i and j are neighboring sites and zero otherwise. The site-diagonal self-energy at the i th site is given by the following (2×2) matrix,

$$\hat{\Sigma}_i(i\omega_n) = \begin{pmatrix} \Sigma_{i\uparrow}(i\omega_n) & S_i(i\omega_n) \\ S_i(i\omega_n) & -\Sigma_{i\downarrow}^*(i\omega_n) \end{pmatrix}, \quad (3)$$

where $\Sigma_\sigma(i\omega_n)$ [$S(i\omega_n)$] is the normal (anomalous) part of the self-energy. In R-DMFT, the self-consistency condition is given by

$$\hat{G}_{lat,ii}(i\omega_n) = \hat{G}_{imp,i}(i\omega_n), \quad (4)$$

where $\hat{G}_{imp,i}$ is the Green's function of the effective impurity model for the i th site. Then the effective medium for each site is given by

$$\hat{G}_i^{-1}(i\omega_n) = [\hat{G}_{imp,i}(i\omega_n)]^{-1} + \hat{\Sigma}_i(i\omega_n). \quad (5)$$

In this paper, we focus on the low energy state without lattice symmetry breaking[56]. In this case, the point group symmetry can be employed to efficiently deduce the lattice Green's function. The inverse lattice Green's function eq. (2) is transformed in terms of a unitary matrix U , as

$$M = U\hat{G}_{lat}^{-1}U^{-1} = \begin{pmatrix} M_{A_{1g}} & 0 & \dots & 0 \\ 0 & M_{A_{2g}} & \dots & 0 \\ \vdots & \vdots & \ddots & 0 \\ 0 & 0 & 0 & M_{T_{2u}} \end{pmatrix}, \quad (6)$$

where M_i is the $(m_i \times m_i)$ matrix, $m_i(\leq L)$ is the number of elements, and i runs over the representations of the group O_h . The lattice Green's function is then obtained by

$$\begin{aligned} \hat{G}_{lat} &= (U^{-1}MU)^{-1} \\ &= U^{-1} \begin{pmatrix} [M_{A_{1g}}]^{-1} & 0 & \dots & 0 \\ 0 & [M_{A_{2g}}]^{-1} & \dots & 0 \\ \vdots & \vdots & \ddots & 0 \\ 0 & 0 & 0 & [M_{T_{2u}}]^{-1} \end{pmatrix} U, \end{aligned} \quad (7)$$

$$\hat{G}_{lat,ii} = \sum_k \sum_{m,n}^{m_k} U_{(km),i} [M_k^{-1}]_{mn} U_{(kn),i} \quad (8)$$

When one considers a system size $r_i \leq 7a$, the total number of sites $L = 1419$. In this case, there are 58 inequivalent sites. Therefore, by solving fifty-eight kinds of effective impurity models and making use of eq. (8), we can iteratively solve the R-DMFT equations and discuss the stability of the polarized superfluid state in the large cluster.

When R-DMFT is applied to our inhomogeneous system, it is necessary to solve a large number of effective impurity models. There are various numerical techniques such as exact diagonalization[57] and the numerical renormalization group [42, 58, 59, 60]. One of the most powerful methods is CTQMC, which has been developed recently. In this method, Monte Carlo samplings of collections of diagrams for the partition function are performed in continuous time. Therefore, the Trotter error, which originates from the Suzuki-Trotter decomposition, is avoided. Furthermore, this method is efficient and applicable to more general classes of models than, for example, the Hirsch-Fye algorithm[61]. The CTQMC method has successfully been applied to various systems such as the Hubbard model [34, 62, 63], the periodic Anderson model [64], the Kondo lattice model [65], and the Holstein-Hubbard model.[66] Here, we use the continuous-time auxiliary field (CTAUX) version of weak-coupling CTQMC [34, 67] to discuss the superfluid state in the optical lattice system. Some details of the CTQMC method are explained in Appendix A.

3. Results

We now consider a three-dimensional optical lattice system with a confining potential to discuss how the superfluid state is realized in this spatially inhomogeneous set-up. In this paper,

we use the hopping integral $t = 1$ as the unit of the energy and fix the confining potential as $V = 0.1$ and the total particle number as $N = 80$. We calculate site-dependent static physical quantities such as the particle density n_i , the pair potential Δ_i and the magnetization m_i , which are defined by

$$n_i = \sum_{\sigma} \langle c_{i\sigma}^{\dagger} c_{i\sigma} \rangle = 2 - \sum_{\sigma} G_{i\sigma}(0_+) \quad (9)$$

$$\Delta_i = \langle c_{i\uparrow} c_{i\downarrow} \rangle = F_i(0_+), \quad (10)$$

$$m_i = \sum_{\sigma} \sigma \langle c_{i\sigma}^{\dagger} c_{i\sigma} \rangle = - \sum_{\sigma} \sigma G_{i\sigma}(0_+). \quad (11)$$

By performing R-DMFT with the CTQMC method, we obtain these quantities first for the balanced system ($N_{\uparrow} = N_{\downarrow} = 40$), as shown in Fig. 1. At high temperatures, particle correlations

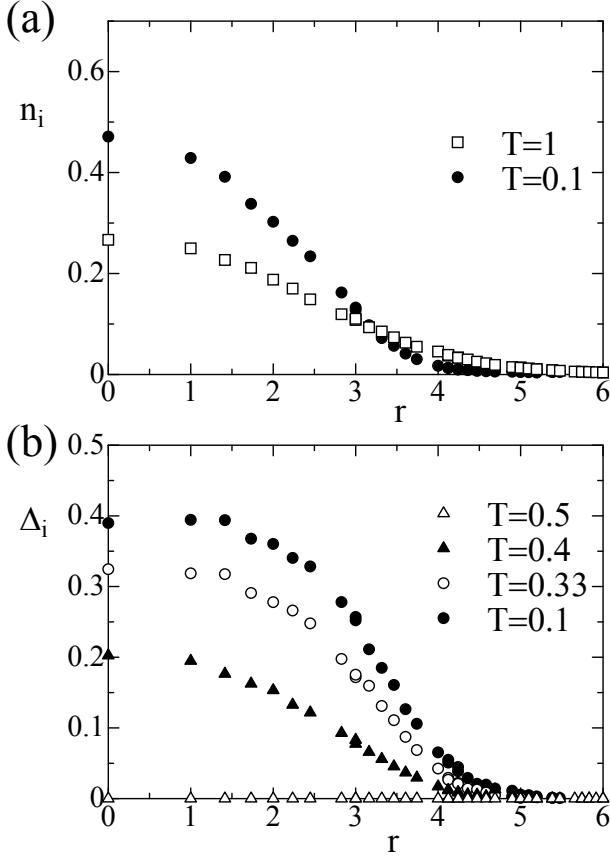


Figure 1: Profiles of particle density $\langle n_{i\sigma} \rangle$ and pair potential Δ_i as a function of r when $V_0 = 0.1$, $U = 8$ and $N_{\uparrow} = N_{\downarrow} = 40$.

are small and kinetic energies high such that the fermions are widely distributed in the trap, as shown in Fig. 1 (a). Decreasing the temperature, the particles gather around the center of the system, which is due to the existence of the attractive interaction. Below a certain critical temperature $T_c = 0.4 \sim 0.5$, the pair potential Δ_i becomes finite, as shown in Fig. 1 (b). This means that a superfluid state is realized in the region with $n_i \neq 0$. It is also found that the magnitude of pair potential depends on the site. This originates from the existence of the harmonic confinement in the system, which is consistent with the results obtained from BdG equations [43].

We next discuss the effect of the imbalanced populations. The obtained results for $P = 0.25$ are shown in Fig. 2, where $P = (N_{\uparrow} - N_{\downarrow}) / (N_{\uparrow} + N_{\downarrow})$ is the spin imbalance parameter. This

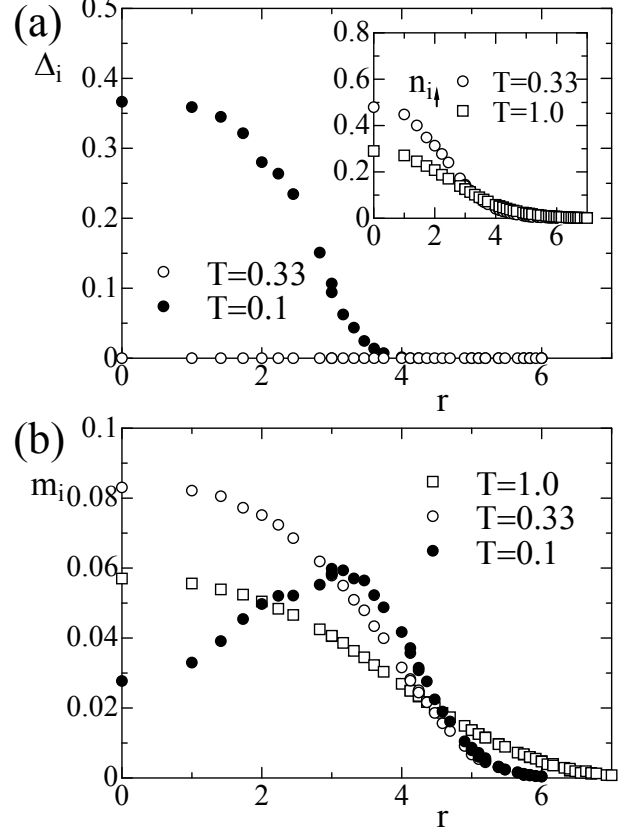


Figure 2: Profiles of pair potential Δ_i and local magnetization m_i as a function of r when $V_0 = 0.1$, $U = 8$, $N_{\uparrow} = 50$ and $N_{\downarrow} = 30$. Inset of (a) shows the profile of particle density $\langle n_{i\uparrow} \rangle$.

case is similar to a system with applied magnetic field. Therefore, the superfluid state should become unstable [34]. In fact, in contrast to the balanced system, the normal metallic state is stabilized even at $T = 0.33$. Further decrease of the temperature ($T = 0.1$) induces the pair potential in a certain region ($r_i < 4a$), as shown in Fig. 2 (a). Since the magnetization is finite in this region, we conclude that the polarized superfluid state is realized in the region ($0 < r_i < 4a$). On the other hand, the normal metallic state still remains in the region ($4a < r_i < 6a$). Note that at $T = 0.1$, the pair potential has a maximum in the center of the system, where particle pairs are strongly formed. As can be seen in Fig. 2 (b), the magnetization at the center of the trap first increases on reducing the temperature. However, when the system becomes superfluid, the magnetization is suppressed and the maximum is pushed to larger values of r_i resulting in a non-monotonic behavior appears in the magnetization curve. It is expected that further decrease of the temperature will lead to a complete suppression of the magnetization near the center of the trap. Detailed calculations will be presented elsewhere.

4. Summary

We have investigated ultracold fermionic atoms trapped in an optical lattice with spin imbalanced populations. By combining the real-space dynamical mean-field theory with continuous-time quantum Monte Carlo simulations based on the Nambu formalism, we have calculated the local particle density, local magnetization, and the pair potential in the system. We have demonstrated how a polarized superfluid state is spatially realized at low temperatures in the model with harmonic confinement.

In this paper, we have studied the stability of the polarized superfluid state in a system with small number of fermions. If the total particle number is larger, the local particle density may increase beyond $n_i = 0.5$. It is known that the density wave state and the superfluid state are degenerate in the homogeneous system at half filling ($n = 0.5$) except in one dimension, which means that a supersolid state might be realizable in an optical lattice system with modulated particle density. It is an interesting problem to clarify this by means of our method. Work along those lines is in progress.

Acknowledgment

The authors thank N. Kawakami for valuable discussions. Parts of the computations were done on TSUBAME Grid Cluster at the Global Scientific Information and Computing Center of the Tokyo Institute of Technology. This work was partly supported by the Grant-in-Aid for Scientific Research 20740194 (A.K.) and the Global COE Program ‘‘Nanoscience and Quantum Physics’’ from the Ministry of Education, Culture, Sports, Science and Technology (MEXT) of Japan. PW acknowledges support from SNF Grant PP002-118866.

Appendix A. Continuous-Time Quantum Monte Carlo simulations in the Nambu Formalism

This appendix explains some details of the CTAUX method [67]. When the superfluid state is discussed in the framework of DMFT, the total particle number is not conserved in the effective Anderson impurity model. The Hamiltonian is then given by

$$H = H_0 + H_U, \quad (\text{A.1})$$

$$H_0 = \sum_{p\sigma} \epsilon_{p\sigma} n_{p\sigma} + \sum_{p\sigma} (V_{p\sigma} d_{\sigma}^{\dagger} a_{p\sigma} + h.c.) + \sum_p (\Delta_p a_{p\uparrow}^{\dagger} a_{p\downarrow}^{\dagger} + h.c.) + \sum_{\sigma} E_{d\sigma} n_{d\sigma}, \quad (\text{A.2})$$

$$H_U = -U \left[n_{d\uparrow} n_{d\downarrow} - \frac{1}{2} (n_{d\uparrow} + n_{d\downarrow} - 1) \right], \quad (\text{A.3})$$

where $a_{p\sigma}$ (d_{σ}) annihilates a fermion with spin σ in the p th orbital of the effective baths (the impurity site). The effective bath is represented by $\epsilon_{p\sigma}$ and Δ_p , and $V_{p\sigma}$ represents the hybridization between the effective bath and the impurity site. $E_{d\sigma}$ is the energy level for the impurity site, $n_{p\sigma} = a_{p\sigma}^{\dagger} a_{p\sigma}$, and

$n_{d\sigma} = d_{\sigma}^{\dagger} d_{\sigma}$. The Green’s function should be defined by the 2×2 matrix, as

$$\hat{G}(\tau) = \begin{pmatrix} G_{\uparrow}(\tau) & F(\tau) \\ F^*(\tau) & -G_{\downarrow}(-\tau) \end{pmatrix}, \quad (\text{A.4})$$

where

$$G_{\sigma}(\tau) = \langle T_{\tau} c_{\sigma}(\tau) c_{\sigma}^{\dagger}(0) \rangle, \quad (\text{A.5})$$

$$F(\tau) = \langle T_{\tau} c_{\uparrow}(\tau) c_{\downarrow}(0) \rangle, \quad (\text{A.6})$$

$$F^*(\tau) = \langle T_{\tau} c_{\downarrow}^{\dagger}(\tau) c_{\uparrow}^{\dagger}(0) \rangle, \quad (\text{A.7})$$

where T_{τ} is the imaginary-time ordering operator and we have chosen the Green’s functions $G_{\sigma}(\tau)$ to be positive.

To perform simulations, we consider here a weak coupling CTQMC approach. The partition function Z is given by

$$Z = \text{Tr} \left[e^{-\beta H_1} T_{\tau} e^{-\int_0^{\beta} d\tau H_2(\tau)} \right] = \sum_{n=0}^{\infty} \int_0^{\beta} d\tau_1 \int_{\tau_1}^{\beta} d\tau_2 \cdots \int_{\tau_{n-1}}^{\beta} d\tau_n \times (-1)^n \text{Tr} \left[e^{-\beta H_1} H_2(\tau_n) H_2(\tau_{n-1}) \cdots H_2(\tau_1) \right], \quad (\text{A.8})$$

where $H_2(\tau) = e^{\tau H_1} H_2 e^{-\tau H_1}$ and $\beta = 1/T$. Here, we have divided the impurity Hamiltonian Eq. (A.1) into two parts as,

$$H_1 = H - H_2, \quad (\text{A.9})$$

$$H_2 = H_U - K/\beta = \frac{K}{2\beta} \sum_{s=-1,1} e^{\gamma s (n_{\uparrow} + n_{\downarrow} - 1)}, \quad (\text{A.10})$$

with $\gamma = \cosh^{-1}(1 + \beta U/2K)$, and K some nonzero constant. In this paper, we set $K = 1$ in the CTQMC simulations. The introduction of the Ising variable s in H_2 enables us to perform simulations at arbitrary filling. An n th order configuration $c = \{s_1, s_2, \dots, s_n; \tau_1, \tau_2, \dots, \tau_n\}$ corresponding to auxiliary spins s_1, s_2, \dots, s_n at imaginary times $\tau_1 < \tau_2 < \dots < \tau_n$ contributes a weight

$$w_c = e^{-K \left(\frac{K d\tau}{2\beta} \right)^n} e^{-\gamma \sum s_i} Z_0 \det \left[\hat{N}^{(n)} \right]^{-1} \quad (\text{A.11})$$

to the partition function. Here, $Z_0 = \text{Tr}[e^{-\beta H_1}]$ and $\hat{N}^{(n)}$ is an $n \times n$ matrix, where each element consists of a 2×2 matrix:

$$\left[\hat{N}^{(n)} \right]^{-1} = \hat{\Gamma}^{(n)} - \hat{g}^{(n)} \left(\hat{\Gamma}^{(n)} - \hat{I}^{(n)} \right), \quad (\text{A.12})$$

$$\hat{I}_{ij}^{(n)} = \delta_{ij} \hat{\sigma}_0, \quad (\text{A.13})$$

$$\hat{\Gamma}_{ij}^{(n)} = \delta_{ij} e^{\gamma s_i} \hat{\sigma}_0, \quad (\text{A.14})$$

$$\hat{g}_{ij}^{(n)} = \begin{pmatrix} g_{0\uparrow}(\tau_i - \tau_j) & f_0(\tau_i - \tau_j) \\ -f_0^*(\tau_i - \tau_j) & g_{0\downarrow}(\tau_j - \tau_i) \end{pmatrix}, \quad (\text{A.15})$$

with $i, j = 1, 2, \dots, n$. The sampling process must satisfy ergodicity and (as a sufficient condition) detailed balance. For ergodicity, it is enough to insert or remove the Ising variables with random orientations at random times to generate all possible configurations.

To satisfy the detailed balance condition, we decompose the transition probability as

$$p(i \rightarrow j) = p^{\text{prop}}(i \rightarrow j) p^{\text{acc}}(i \rightarrow j), \quad (\text{A.16})$$

where $p^{\text{prop}}(p^{\text{acc}})$ is the probability to propose (accept) the transition from the configuration i to the configuration j . Here, we consider the insertion and removal of the Ising spins as one step of the simulation process, which corresponds to a change of ± 1 in the perturbation order. The probability of insertion/removal of an Ising spin is then given by

$$p^{\text{prop}}(n \rightarrow n+1) = \frac{d\tau}{2\beta}, \quad (\text{A.17})$$

$$p^{\text{prop}}(n+1 \rightarrow n) = \frac{1}{n+1}. \quad (\text{A.18})$$

For this choice, the ratio of the acceptance probabilities becomes

$$\frac{p^{\text{acc}}(n \rightarrow n+1)}{p^{\text{acc}}(n+1 \rightarrow n)} = \frac{K}{n+1} e^{-\gamma s_{n+1}} \frac{\det N^{(n)}}{\det N^{(n+1)}}. \quad (\text{A.19})$$

When the Metropolis algorithm is used to sample the configurations, we accept the transition from n to $n \pm 1$ with the probability

$$\min \left[1, \frac{p^{\text{acc}}(n \rightarrow n \pm 1)}{p^{\text{acc}}(n \pm 1 \rightarrow n)} \right]. \quad (\text{A.20})$$

In each Monte Carlo step, we measure the following Green's functions ($0 < \tau < \beta$),

$$G_{\sigma}(\tau) = \frac{1}{Z} \text{Tr} \left[e^{-\beta H} c_{\sigma}(\tau) c_{\sigma}^{\dagger}(0) \right], \quad (\text{A.21})$$

$$F(\tau) = \frac{1}{Z} \text{Tr} \left[e^{-\beta H} c_{\uparrow}(\tau) c_{\downarrow}(0) \right], \quad (\text{A.22})$$

$$F^*(\tau) = \frac{1}{Z} \text{Tr} \left[e^{-\beta H} c_{\downarrow}^{\dagger}(\tau) c_{\uparrow}^{\dagger}(0) \right]. \quad (\text{A.23})$$

By using Wick's theorem, the contribution of a certain configuration c is given by

$$G_{\sigma}^c(\tau) = \det[N^{(n)}] \det \begin{pmatrix} [N^{(n)}]^{-1} & Q_{\sigma} \\ R_{\sigma} & g_{0\sigma}(\tau) \end{pmatrix}, \quad (\text{A.24})$$

$$F^c(\tau) = \det[N^{(n)}] \det \begin{pmatrix} [N^{(n)}]^{-1} & Q' \\ R' & f_0(\tau) \end{pmatrix}, \quad (\text{A.25})$$

$$F^{*c}(\tau) = \det[N^{(n)}] \det \begin{pmatrix} [N^{(n)}]^{-1} & Q^{*'} \\ R^{*'} & f_0^*(\tau) \end{pmatrix}, \quad (\text{A.26})$$

where $Q_{\sigma}, Q', Q^{*'}, R_{\sigma}, R', R^{*'}$ are vectors, in which the i th element ($i = 1, 2, \dots, n$) is defined by

$$Q_{\uparrow i} = \{-g_{0\uparrow}(\tau_i) f_0^*(\tau_i)\}^T, \quad (\text{A.27})$$

$$Q_{\downarrow i} = \{f_0(\tau_i - \tau) g_{0\downarrow}(\tau - \tau_i)\}^T, \quad (\text{A.28})$$

$$Q'_i = \{-f_0(\tau_i) - g_{0\downarrow}(-\tau_i)\}^T, \quad (\text{A.29})$$

$$Q_i^{*'} = Q_{\uparrow i}, \quad (\text{A.30})$$

$$R_{\uparrow i} = (e^{\gamma s_i} - 1) \{g_{0\uparrow}(\tau - \tau_i) f_0(\tau - \tau_i)\}, \quad (\text{A.31})$$

$$R_{\downarrow i} = (e^{\gamma s_i} - 1) \{f_0^*(-\tau_i) - g_{0\downarrow}(\tau_i)\}, \quad (\text{A.32})$$

$$R'_i = R_{\uparrow i}, \quad (\text{A.33})$$

$$R_i^{*'} = (e^{\gamma s_i} - 1) \{f_0^*(\tau - \tau_i) - g_{0\downarrow}(\tau_i - \tau)\}. \quad (\text{A.34})$$

References

- [1] M. H. Anderson, J. R. Ensher, M. R. Matthews, C. E. Wieman, and E. A. Cornell: *Science* **269** (1995) 198.
- [2] K. B. Davis, M.-O. Mewes, M. R. Andrews, N. J. van Druten, D. S. Durfee, D. M. Kurn, and W. Ketterle: *Phys. Rev. Lett.* **75**, 3969 (1995).
- [3] For a review, see *Nature (London)* **416** (2002) 205-246.
- [4] C. J. Pethick and H. Smith, *Bose-Einstein Condensation in Dilute Gases* (Cambridge University Press, Cambridge, 2002).
- [5] L. Pitaevskii and S. Stringari, *Bose-Einstein Condensation* (Clarendon Press, Oxford, 2003).
- [6] I. Bloch and M. Greiner: *Advances in Atomic, Molecular, and Optical Physics*, edited by P. Berman and C. Lin (Academic Press, New York, 2005), Vol. 52 p. 1.
- [7] I. Bloch: *Nature Physics* **1** (2005) 23.
- [8] D. Jaksch and P. Zoller: *Ann. Phys. (NY)* **315** (2005) 52.
- [9] O. Morsch and M. Oberhaller: *Rev. Mod. Phys.* **78** (2006) 179.
- [10] M. Greiner, O. Mandel, T. Esslinger, T. W. Hänsch and I. Bloch: *Nature* **415** (2003) 39.
- [11] J. K. Chin, D. E. Miller, Y. Liu, C. Stan, W. Setiawan, C. Sanner, K. Xu, and W. Ketterle: *Nature* **443** (2006) 961.
- [12] R. Jördens, N. Strohmaier, K. Günter, H. Moritz, T. Esslinger, *Nature* **455** (2008) 204.
- [13] U. Schneider, L. Hackermüller, S. Will, Th. Best, I. Bloch, T. A. Costi, R. W. Helmes, D. Rasch, A. Rosch: *Science* **322** (2008) 1520.
- [14] M. W. Zwierlein, A. Schirotzek, C. H. Shunck, and W. Ketterle: *Science* **311** (2006) 492.
- [15] G. B. Partridge, W. Li, R. I. Kamar, Y. Liao, and R. G. Hulet: *Science* **311** (2006) 503.
- [16] P. Fulde and R. A. Ferrell: *Phys. Rev.* **135** (1964) A550.
- [17] A. I. Larkin and Y. N. Ovchinnikov: *Sov. Phys. JETP* **20** (1965) 762.
- [18] H. A. Radovan, N. A. Fortune, T. P. Murphy, S. T. Hannahs, E. C. Palm, S. W. Tozer, and D. Hall: *Nature* **425** (2003) 51.
- [19] A. Bianchi, R. Movshovich, C. Capan, P. G. Pagliuso, and J. L. Sarrao: *Phys. Rev. Lett.* **91** (2003) 187004.
- [20] Y. Matsuda and H. Shimahara: *J. Phys. Soc. Jpn.* **76** (2007) 051005
- [21] H. Adachi and R. Ikeda: *Phys. Rev. B* **68** (2003) 184510; K. Miyake: *J. Phys. Soc. Jpn.* **77** (2008) 123703; Y. Yanase and M. Sigrist: *J. Phys. Soc. Jpn.* **78** (2009) 114715; D. F. Agterberg, M. Sigrist, and H. Tsunetsugu: *Phys. Rev. Lett.* **102** (2009) 207004.
- [22] T. K. Koponen, T. Paananen, J.-P. Martikainen, and P. Törmä: *Phys. Rev. Lett.* **99** (2007) 120403; H. Tamaki, K. Miyake, and Y. Ohashi: *J. Phys. Soc. Jpn.* **78** (2009) 073001.
- [23] M. Tezuka and M. Ueda: *Phys. Rev. Lett.* **100** (2008) 110403; M. Machida, S. Yamada, M. Okumura, Y. Ohashi, and H. Matsumoto: *Phys. Rev. A* **77** (2008) 053614.
- [24] G. Sarma: *J. Phys. Chem. Solids* **24** (1963) 1029.
- [25] W. V. Liu and F. Wilczek: *Phys. Rev. Lett.* **90** (2003) 047002.
- [26] D. E. Sheehy and L. Radzihovsky: *Phys. Rev. Lett.* **96** (2006) 060401.
- [27] D. T. Son and M. A. Stephanov: *Phys. Rev. A* **74** (2006) 013614.
- [28] S. Pilati and S. Giorgini: *Phys. Rev. Lett.* **100** (2008) 030401.
- [29] W. Metzner and D. Vollhardt: *Phys. Rev. Lett.* **62** (1989) 324.
- [30] E. Müller-Hartmann: *Z. Phys. B* **74** (1989) 507.
- [31] A. Georges, G. Kotliar, W. Krauth and M. J. Rozenberg: *Rev. Mod. Phys.* **68** (1996) 13.
- [32] T. Pruschke, M. Jarrell, and J. K. Freericks: *Adv. Phys.* **44** (1995) 187.
- [33] A. N. Rubtsov, V. V. Savkin and A. I. Lichtenstein: *Phys. Rev. B* **72** (2005) 035122.
- [34] A. Koga and P. Werner, *J. Phys. Soc. Jpn.* **79** (2010) 064401.
- [35] R. T. Scalettar, E. Y. Loh, J. E. Gubernatis, A. Moreo, S. R. White, D. J. Scalapino, R. L. Sugar, and E. Dagotto: *Phys. Rev. Lett.* **62** (1989) 1407.
- [36] R. Micnas, J. Ranninger, and S. Robaszkiewicz: *Rev. Mod. Phys.* **62** (1990) 113.
- [37] J. K. Freericks, M. Jarrell and M. J. Scalapino: *Phys. Rev. B* **48** (1993) 6302.
- [38] M. Keller, W. Metzner, and U. Schollwöck: *Phys. Rev. Lett.* **86** (2001) 4612.
- [39] M. Capone, C. Castellani, and M. Grilli: *Phys. Rev. Lett.* **88** (2002) 126403.
- [40] A. Garg, H. R. Krishnamurthy, and M. Randeria: *Phys. Rev. B* **72** (2005) 024517.
- [41] A. Toschi, M. Capone, and C. Castellani: *Phys. Rev. B* **72** (2005) 235118.

- [42] J. Bauer, A. C. Hewson, and N. Dupuis: Phys. Rev. B **79** (2009) 214518; J. Bauer and A. C. Hewson: Europhys. Lett. **85** (2009) 27001.
- [43] Y. Chen, Z. D. Wang, F. C. Zhang, and C. S. Ting: Phys. Rev. B **79** (2009) 054512; Y. Yanase, Phys. Rev. B **80**, 220510 (2009).
- [44] M. Yamashita and M. W. Jack: Phys. Rev. A **76** (2007) 023606.
- [45] A. Rüegg, S. Pilgram, and M. Sigrist: Phys. Rev. B **75** (2007) 195117.
- [46] Y. Fujihara, A. Koga, and N. Kawakami: Phys. Rev. A **79** (2009) 013610.
- [47] T.-L. Dao, M. Ferrero, A. Georges, M. Capone, and O. Parcollet: Phys. Rev. Lett. **101** (2008) 236405.
- [48] M. Machida, S. Yamada, Y. Ohashi, and H. Matsumoto: Phys. Rev. A **74** (2006) 053621.
- [49] G. Xianlong, M. Rizzi, M. Polini, R. Fazio, M. P. Tosi, V. L. Campo Jr., and K. Capelle: Phys. Rev. Lett. **98** (2007) 030404.
- [50] M. Rigol, A. Muramatsu, G. G. Batrouni and R. T. Scalettar, Phys. Rev. Lett. **91** (2003) 130403.
- [51] F. K. Pour, M. Rigol, S. Wessel, and A. Muramatsu: Phys. Rev. B **75** (2007) 161104.
- [52] M. Pothoff and W. Nolting: Phys. Rev. B **59** (1999) 2549.
- [53] S. Okamoto and A. J. Millis: Phys. Rev. B **70** (2004) 241104(R); Nature (London) **428** (2004) 630.
- [54] R. W. Helmes, T. A. Costi and A. Rosch: Phys. Rev. Lett. **100** (2008) 056403.
- [55] M. Snoek, I. Titvinidze, C. Töke, K. Byczuk, and W. Hofstetter: New. J. Phys. **10** (2008) 093008.
- [56] A. Koga, T. Higashiyama, K. Inaba, S. Suga, and N. Kawakami: J. Phys. Soc. Jpn. **77** (2008) 073602; Phys. Rev. A **79** (2009) 013607.
- [57] M. Caffarel and W. Krauth: Phys. Rev. Lett. **72** (1994) 1545.
- [58] H. R. Krishna-murthy, J. W. Wilkins, and K. G. Wilson: Phys. Rev. B **21** (1980) 1003.
- [59] R. Bulla, T. Costi, and Th. Pruschke: Rev. Mod. Phys. **80** (2008) 395.
- [60] O. Sakai and Y. Kuramoto: Solid State Comm. **89** (1994) 307.
- [61] J. E. Hirsch and R. M. Fye, Phys. Rev. Lett. **56**, 2521 (1986).
- [62] P. Werner, A. Comanac, L. de' Medici, M. Troyer, and A. J. Millis: Phys. Rev. Lett. **97** (2006) 076405; P. Werner and A. J. Millis: Phys. Rev. B **75** (2007) 085108;
- [63] P. Werner and A. J. Millis: Phys. Rev. B **74** (2006) 155107; Phys. Rev. Lett. **99** (2007) 126405; P. Werner, E. Gull, and A. J. Millis: Phys. Rev. B **79** (2009) 115119.
- [64] D. J. Luitz and F. F. Assaad: Phys. Rev. B **81** (2010) 024509.
- [65] J. Otsuki, H. Kusunose, P. Werner, and Y. Kuramoto: J. Phys. Soc. Jpn. **76** (2007) 114707; J. Otsuki, H. Kusunose, and Y. Kuramoto: Phys. Rev. Lett. **102** (2009) 017202.
- [66] F. F. Assaad and T. C. Lang: Phys. Rev. B **76** (2007) 035116; P. Werner and A. J. Millis: Phys. Rev. Lett. **99** (2007) 146404.
- [67] E. Gull, P. Werner, O. Parcollet and M. Troyer: Europhys. Lett. **82** (2008) 57003.